Supplementary Information

Design of the core-shell catalyst: an effective strategy for suppressing side reactions in syngas to light olefins direct selective conversion

Li Tan[a,b], Fan Wang[c], Peipei Zhang[b], Yuichi Suzuki[b], Yingquan Wu[d], Jiangang Chen[d], Guohui Yang[b,d,] and Noritatsu Tsubaki[b,*]*

[a] Institute of Molecular Catalysis and Operando Characterization, State Key Laboratory of Photocatalysis on Energy and Environment, College of Chemistry, Fuzhou University, Fuzhou, 350108, China

[b] Department of Applied Chemistry, School of Engineering, University of Toyama, Gofuku 3190, Toyama 930-8555, Japan

[c] Leibniz-Institut für Katalyse e.V. an der Universität Rostock, Albert-Einstein Strasse 29a, 18059 Rostock, Germany

[d] State Key Laboratory of Coal Conversion, Institute of Coal Chemistry, Chinese Academy of Sciences, Taiyuan, 030001, China.

***Corresponding author:** tsubaki@eng.u-toyama.ac.jp (Noritatsu Tsubaki)

thomas@eng.u-toyama.ac.jp (Guohui Yang),

Materials and Methods

1. Catalyst preparation:

The Zn-Cr catalyst was synthesized through a typical co-precipitation method by mixing solution of $Cr(NO_3)_3 \cdot 9H_2O$ and $Zn(NO_3)_2 \cdot 6H_2O$ (Zn: Cr= 3:1 in molar) with $(NH_4)_2CO_3$ aqueous solution as the precipitant. Precipitation process was performed at 60 °C and pH=7.0-8.0 in a well-stirred container. The precipitate was first aged at room temperature for 24 h, and then washed with deionized water until pH = 7.0. After the followed drying at 120 °C for 12 h, the dried precipitate was further calcined at 350 °C for 6 h to obtain the final catalyst, denoted as Zn-Cr. The samples were granulated to 40-60 meshes.

The SAPO-34 zeolite was synthesized using a hydrothermal method. Aluminum isopropoxide, silica sol (30%), phosphoric acid (85%) and distilled water were mixed and stirred at room temperature. DEA (Diethylamine) was added 1 h later and the resulting mixture was stirred until homogeneous. The gel was heated and crystallized at 200 °C for 24 h. The typical molar composition of the gel was $2.0DEA: 0.6SiO_2: 1.0Al_2O_3: 0.8P_2O_5: 50H_2O$. After crystallization, the as-synthesized sample was obtained after centrifugal separation, washing and drying in air at 120 °C. At last the sample calcined at 550 °C for 5 h, denoted as SAPO. The samples were granulated to 40-60 meshes.

The diluted silica sol, as binder, was used to moisten the Zn-Cr core catalyst. And then the prepared SAPO-34 zeolite powder was mixed with the soaked Zn-Cr core catalyst (40-60 meshes) in a round bottomed flask, followed by vigorously shaking. The obtained sample was finally treated by calcination at 500 °C for 2 h increasing the mechanical strength of zeolite shell, denoted as Zn-Cr@SAPO.

The physical mixture catalyst (40-60 meshes) of Zn-Cr and SAPO was prepared by a typical physical mixture method as reference catalyst with the same weight ratio to that of Zn-Cr@SAPO, denoted as Zn-Cr+SAPO.

Two samples were prepared and studied to verify the effects from the silica sol. The Zn-Cr catalyst and SAPO-34 zeolite were moistened separately by the diluted silica

sol, followed by drying and calcining. The samples were granulated to 40-60 meshes. The two samples were denoted as Zn-Cr@SiO_2 and SAPO@SiO_2, respectively.

2. Catalytic reaction tests:

The catalyst evaluation experiments were carried out in a fixed-bed tubular reactor packed with 0.5 g catalyst. The flow rate of feed gas was controlled by a mass flow controller. The catalyst was subjected to in situ reduction in H_2 for 10 h at 400 °C prior to reaction. After the reduction process, syngas was introduced into the reactor for reaction. The reaction conditions were as follows: H_2/CO=2.0, reaction time=4 h, reaction pressure of 2.0 or 5.0 MPa, space velocity from 2160 to 6480 $cm^3h^{-1}g_{cat}^{-1}$ and reaction temperature from 300 to 450 ^oC. The typical composition of syngas was H_2 63.6%, CO 33.2%, Ar 3.2%.

Syngas and exit gas were analyzed by a gas chromatograph equipped with a column of carbon sieves and a thermal conductivity detector (TCD) for the contents of CH_4, CO and CO_2. Methanol, DME and hydrocarbons up to C_8 were analyzed by a gas chromatograph equipped with a flame ionization detector (FID). CH_4 was taken as a reference bridge between FID and TCD. CO conversion was calculated on a carbon atom basis, i.e.

(1) C_{CO}=（$X_{CO,\,in}$ - $X_{CO,\,out}$）/ ($X_{CO,\,in}$) ×100%

C_{CO}- Conversion of CO, %;

$X_{CO,\,in}$-Mole fraction of CO in pristine syngas;

$X_{CO,\,out}$-Mole fraction of CO in exit gas;

(2) Sel_{CO2}=$X_{CO2,out}$/ ($X_{CO,\,in}$ - $X_{CO,\,out}$) ×100%

Sel_{CO2}- Selectivity of CO, %;

$X_{CO2,\,out}$- Mole fraction of CO_2 in exit gas;

(3) $$Sel_i = \frac{R_{i,s} f_{i,m}}{\sum_i R_{i,s} f_{i,m}}$$

Sel_i- Selectivity of component i, %;

$R_{i,\,s}$- Area ratio of hydrocarbon in chromatogram;

$f_{i,\,m}$- Correction of mass.

3. Catalyst characterization:

The crystalline structure of the sample was measured by X-ray diffraction (XRD) with a Rigaku RINT 2400 diffractometer employing Cu Kα radiation. All samples were scanned at 40 kV and 40 mA in the range of 5-80^{o}. The Thermodynamic chart images of the sample was obtained by a Two-dimensional X-ray (2D-XRD) with a Rigaku Hypix-400 detector. We used 2D slit 0.5mm for Cu of incident soller slit. The camera length was 148.578 mm.

The acidity of catalysts was studied by the temperature programmed desorption (TPD) with BELCAT-B-TT (BEL JAPAN INC.) using NH_3. TPD of NH_3 was carried out between 50 and 800 °C under a helium flow (30 ml/min) with a heating rate of 10 °C/min. Before the test, the samples were pretreated under helium atmosphere at 500 ^{o}C for 1 h, then, cooled to 50 °C, and exposed to pure NH_3 (30 ml/min) for 0.5 h.

Nitrogen adsorption measurements were carried out with a Quantachrome Instruments AUTOSORB-1, and BET surface area and the pore size distribution were determined from the isotherms. The samples were outgassed at 200 ^{o}C for 2 h before each test.

The surface morphology and elemental composition were obtained by field-emission scanning electron microscope (FE-SEM, JEOL JSM-6700F) and scanning electron microscope (SEM, JEOL JSM-6360LV) with JED-2300 energy dispersive spectroscopy (EDS) attachment. The samples were per-treated in vacuum at 343 K overnight and sprayed platinum at 10 kv for 200 s before examination.

The H_2 temperature programmed reduction (H_2-TPR) profiles were recorded in a fixed-bed reactor system equipped with a thermal conductivity detector. The catalyst (100 mg) was pretreated at 400 ^{o}C under Ar flow (40 ml/min) and then cooled down to 50 ^{o}C under Ar flow. Then H_2–N_2 (10:90) was introduced into the analysis system. H_2-TPR profiles were recorded at a temperature rising rate of 5 ^{o}C / min from 50 ^{o}C to 600 ^{o}C.

The fluorescence intensity maps were measured by X-ray fluorescence CT (XRF-CT) with a fluorescence detector (Vertex EX-90). The source light generated by the undulator was sized at 5 μm (horizontal) and 5 μm (vertical) with 20 keV. The sample

was scanned by horizontal, angular and vertical triple cycle scanning. The matrix can be transformed into the intensity distribution of the fluorescence signal in the horizontal plane of the incident light. Then the distribution images of different elements can be obtained by filling the integrals of these fluorescence peaks into the matrix elements mentioned above. In the experiment, a total of 260 points were collected with 10um horizontal step; 37 points with 180° were scanned with 5° angle; and 9 points were collected with 10um vertical step. The integral time of each point was 0.2 second, the residence time (stability) time of the motor was 0.2 second, plus the motor motion time, each data point took about 0.7 second. The collection time of each section was about 2 hour, and the total experiment time was nearly 1 day. At last, by changing the vertical direction and directing the incident light to different positions of the sample, the cross-section element distribution images of the samples with different positions can be obtained. By superimposing these cross sections, the three-dimensional distribution image of elements can be obtained.

The X-ray photoelectron spectroscopy (XPS) analysis was accomplished by Thermo Fisher Scientific ESCALAB 250Xi multifunctional X-ray photoelectron spectroscope, by which to determine the existence of Cr, Zn and oxygen state on the outward appearance of catalysts. The data processing was performed using Avantage software.

The inductive coupled plasma atomic emission spectrometry (ICP-AES) was employed to determine the real Zn-Cr/SAPO ratio of the catalytsts using Perkin Elmer Optima 7300DV atomic emission spectrometry spectrometer.

The in situ FT-IR spectra were recorded with a Bruker Tensor 27 with a MCT detector at the 4000-800 cm^{-1} range, with a resolution of 4 cm^{-1} and 64 acquisition scans. The catalyst was reduced by H_2 in prior to the test. After pretreating by Ar, C_2H_4 and C_3H_6 were introduced for adsorption at 300 or 400 ^oC under 2 MPa or atmospheric pressure, respectively, then after pressure rapidly released, the catalyst was under a flow of Ar for desorption for 6 or 10 min. Ultimately, the temperature was cooled down in Ar, and the CO_2 formation on catalysts was investigated under a flow of syngas at 300 or 400 ^oC under 2 MPa or atmospheric pressure, respectively.

The catalysts carbon deposition behavior was investigated by thermo gravimetric analysis (DTA/TGA-60, Shimadzu). The samples were heated at a rate of 10 ^{o}C/min from room temperature to 800 ^{o}C in air flow.

Raman spectra were recorded with a Renishaw inVia 2000 Raman microscope by using an Ar^{+} ion laser at 514.5 nm wavelength.

The diffuse reflectance (DR) UV–vis spectra of used catalysts were recorded on an Agilent Cary 5000 UV–vis–NIR spectrophotometer

4. Theoretical Calculations

All calculations were conducted by using the plane-wave based density functional theory (DFT) method implemented in the Vienna ab initio simulation package (VASP). The interaction of electron and ion was described by the projector augmented wave (PAW) method.[1] The electron exchange and correlation energy were treated within the generalized gradient approximation in the Perdew-Burke-Ernzerhof formalism (GGA-PBE).[2] To have accurate energies with errors less than 1 meV per atom, a cutoff energy of 400 eV and the Gaussian electron smearing method with σ = 0.10 eV were used. Geometry optimization was converged until the forces acting on the atoms were smaller than 0.05 eV/Å, whereas the energy threshold-defining self-consistency of the electron density was set to 10^{-4} eV. The adsorption energy (E_{ads}) was calculated by subtracting the energies of gas-phase species and the clean surface from the total energy of the adsorbed species (X), E_{ads} = E(X/slab) – [E(X) + E(slab)], where E(X/slab) is the total energy of the slab with one X molecule, E(slab) is the total energy of the bare slab and E(X) is the total energy of a free X molecule in gas phase. Therefore, the more negative the E_{ads} the stronger the adsorption. The calculated energies also included the zero-point energy (ZPE) which was calculated based on the molecular vibration analysis.[3] For H-SAPO34, the methods DFT-D3 was adopted to correct van der Waals (vdW) interaction. A 3×3×3 Monkhorst-Pack k-point grid was used for sampling the Brillouin zone. A model of spinel $ZnCr_2O_4$(111) surface with 12 atomic layers (with the top six layers relaxed and the bottom six layers fixed) and the vacuum thickness of 20 Å were used to study all adsorption process. A 3×3×1 Monkhorst-Pack k-point grid was utilized for sampling the Brillouin zone.

Table S1. Catalytic data in CO hydrogenation of different space velocity. [a]

Catalyst	SV	CO	CO_2	Products distribution (%) [b]								
	($cm^3h^{-1}g_{cat}^{-1}$)	Con. (%)	Sel.(%)	MeOH	CH_4	C_2H_6	C_3~C_4	C_2~$C_4^=$	$C_5^=$	n-C_5	i-C_5	others
Zn-Cr	2160	17.71	47.14	3.81	59.86	14.15	6.34	13.80	0.61	1.31	0.13	0
	4320	8.55	48.82	6.82	55.68	8.91	4.18	22.57	0.55	0.98	0.31	0
	6480	5.60	49.86	8.82	56.19	7.03	3.36	23.01	0.49	0.84	0.26	0
Zn-Cr+SAPO-2 steps[c]	2160	22.28	41.53	5.66	52.05	12.58	12.10	15.69	0.48	1.15	0.10	0.19
	4320	10.76	47.52	6.70	49.56	10.64	7.54	24.04	0.53	0.88	0.10	0
	6480	7.76	45.50	4.45	52.58	8.33	5.63	27.86	0.44	0.71	0	0
Zn-Cr+SAPO[c]	2160	30.39	45.89	0.09	11.46	16.32	47.70	19.74	1.49	2.31	0.05	0.83
	4320	14.50	45.88	0.27	13.18	11.83	37.91	33.56	1.58	1.67	0	0
	6480	9.82	46.92	0.56	14.30	9.02	33.54	39.70	1.50	1.38	0	0
Zn-Cr@SAPO[c]	2160	31.41	36.58	0.03	8.90	10.29	31.74	45.28	1.27	2.09	0.08	0.32
	4320	16.85	35.83	0.18	9.15	7.69	24.81	55.53	1.28	1.36	0	0
	6480	10.69	36.16	0.42	8.39	6.32	18.33	64.31	1.15	1.08	0	0

[a] Reaction condition: H_2/CO=2.0, P=2.0 MPa, T=400 °C, Reaction time =4 h. [b] All the products except CO_2. [c] The weight ratio of ZnCr and SAPO is 4:1.

Table S2. Catalytic data in CO hydrogenation of different temperature under 2.0 MPa. [a]

Catalyst	Temp.	CO	CO_2	Products distribution (%)[b]								
	(°C)	Con.(%)	Sel.(%)	MeOH	CH_4	C_2H_6	C_3~C_4	C_2~$C_4^=$	$C_5^=$	n-C_5	i-C_5	others
Zn-Cr	300	3.47	34.91	92.58	4.32	0.37	0.31	2.42	0	0	0	0
	350	3.53	43.91	49.92	30.05	3.62	1.71	13.65	0.56	0.48	0	0
	400	5.60	49.86	8.82	56.19	7.03	3.36	23.01	0.49	0.84	0.26	0
	450	10.99	44.17	0.77	60.56	13.21	5.76	17.88	0.67	1.00	0.14	0
Zn-Cr+SAPO-2 steps[c]	300	2.08	29.90	80.41	9.87	1.06	0.23	7.90	0	0	0	0.53
	350	4.80	30.14	49.76	26.81	4.61	2.93	13.75	0.50	0.67	0	0.97
	400	7.76	45.50	4.45	52.58	8.33	5.63	27.86	0.44	0.71	0	0
	450	15.60	44.58	2.28	58.90	13.14	8.54	15.63	0.48	0.92	0.12	0
Zn-Cr+SAPO[c]	300	3.44	12.11	65.30	11.21	0.54	3.56	19.39	0	0	0	0
	350	6.18	25.36	43.45	14.17	3.57	12.34	23.21	1.22	1.32	0	0.72
	400	9.82	46.92	0.56	14.30	9.02	33.54	39.70	1.50	1.38	0	0
	450	11.18	47.96	0.22	54.04	18.32	14.27	10.69	0.68	1.71	0.07	0
Zn-Cr@SAPO[c]	300	3.92	6.44	73.83	6.13	0.31	1.14	18.16	0.44	0	0	0
	350	6.19	18.41	37.89	7.67	11.86	5.71	35.25	1.02	0.60	0	0
	400	10.69	36.16	0.42	8.39	6.32	18.33	64.31	1.15	1.08	0	0
	450	12.99	40.35	0	49.08	19.32	10.61	17.97	0.60	2.08	0.11	0.24

[a] Reaction condition: $H_2/CO=2.0$, P=2.0 MPa, Space velocity=6480 $cm^3h^{-1}g_{cat}^{-1}$, Reaction time =4 h.

[b] All the products except CO_2. [c] The weight ratio of ZnCr and SAPO is 4:1.

Table S3. Catalytic data in CO hydrogenation of different temperature under 5.0 MPa. [a]

Catalyst	Temp.	CO	CO_2	Products distribution (%)[b]								
	(°C)	Con.(%)	Sel.(%)	MeOH	CH_4	C_2H_6	C_3~C_4	C_2~$C_4^=$	$C_5^=$	n-C_5	i-C_5	others
Zn-Cr	300	4.46	35.12	82.98	7.80	1.52	1.37	5.32	0.39	0.27	0	0.35
	350	10.69	48.50	60.91	21.62	5.76	2.64	7.83	0.51	0.54	0.05	0.15
	400	11.94	44.52	23.57	52.31	11.89	4.18	7.15	0.30	0.52	0.07	0
	450	19.83	45.89	2.98	67.87	15.33	6.27	6.45	0.30	0.62	0.14	0.04
Zn-Cr+SAPO-2 steps[c]	300	5.79	19.57	75.89	10.17	1.64	2.37	8.88	0.59	0.35	0	0.10
	350	11.31	35.64	68.61	13.52	5.55	4.74	6.67	0.23	0.46	0.22	0
	400	13.55	45.88	8.66	54.13	12.67	14.66	8.96	0.21	0.44	0.06	0.12
	450	24.38	46.76	1.33	60.23	9.45	19.72	8.15	0.13	0.43	0.11	0.45
Zn-Cr+SAPO[c]	300	5.79	19.57	75.89	10.17	1.64	2.37	8.88	0.59	0.35	0	0.10
	350	11.31	25.64	68.61	13.52	5.55	4.74	6.67	0.23	0.46	0.22	0
	400	25.73	44.13	2.26	15.16	15.96	35.59	20.23	0.74	0.92	0.05	0.10
	450	31.41	48.38	0.18	45.95	17.93	27.38	5.58	0.46	2.12	0.07	0.32
Zn-Cr@SAPO[c]	300	6.79	11.66	75.54	12.41	2.60	3.74	5.06	0.25	0.40	0	0
	350	11.80	20.49	65.70	13.15	3.74	5.78	1.95	0.34	0.34	0	0
	400	26.35	39.12	5.88	18.97	13.55	37.40	22.69	0.61	0.85	0.05	0
	450	40.71	42.03	0.05	54.06	10.18	16.46	16.02	0.36	2.39	0.14	0.34

[a] Reaction condition: H_2/CO=2.0, P=5.0 MPa, Space velocity=6480 $cm^3h^{-1}g_{cat}^{-1}$, Reaction time =4 h.

[b] All the products except CO_2. [c] The weight ratio of ZnCr and SAPO is 4:1.

Table S4. Texture parameters of varied catalysts.

Sample	Surface Area(m^2/g)[a]	Pore Volume (cm^3/g) [a]	Average Pore Diameter (nm) [a]	Zn-Cr/SAPO weight ratio [b]
Zn-Cr	81.5	0.36	17.63	/
SAPO	308.0	0.11	1.45	/
Zn-Cr@SAPO	226.2	0.52	9.15	4:1

[a] Calculated by BET method. [b] Measured by ICP-AES.

Table S5. Catalytic data in CO hydrogenation of different H_2/CO ratios. [a]

Catalyst	H_2/CO	CO Con. (%)	CO_2 Sel.(%)	Products distribution (%)[b]								
				MeOH	CH_4	C_2H_6	C_3~C_4	C_2~$C_4^=$	$C_5^=$	n-C_5	i-C_5	others
Zn-Cr@SAPO[c]	2	10.69	36.16	0.42	8.39	6.32	18.33	64.31	1.15	1.08	0	0
Zn-Cr@SAPO[c]	1	8.99	36.01	0.55	18.45	7.99	15.41	55.79	0.98	0.83	0	0

[a] Reaction condition: Space velocity=6480 $cm^3h^{-1}g_{cat}^{-1}$, P=2.0 MPa, T=400 ^oC, Reaction time =4 h.

[b] All the products except CO_2. [c] The weight ratio of ZnCr and SAPO is 4:1.

Table S6. Catalytic data in CO hydrogenation of different catalysts. [a]

Catalyst	CO	CO_2	Products distribution (%)[b]								
	Con. (%)	Sel.(%)	MeOH	CH_4	C_2H_6	C_3~C_4	C_2~$C_4^=$	$C_5^=$	n-C_5	i-C_5	others
Zn-Cr+SAPO[c]	9.82	46.92	0.56	14.30	9.02	33.54	39.70	1.50	1.38	0	0
Zn-Cr@SiO_2+SAPO@SiO_2[c]	9.66	47.12	0.55	14.45	7.99	35.41	38.79	1.41	1.40	0	0

[a] Reaction condition: Space velocity=6480 $cm^3h^{-1}g_{cat}^{-1}$, P=2.0 MPa, T=400 °C, Reaction time =4 h.

[b] All the products except CO_2. [c] The weight ratio of ZnCr and SAPO is 4:1.

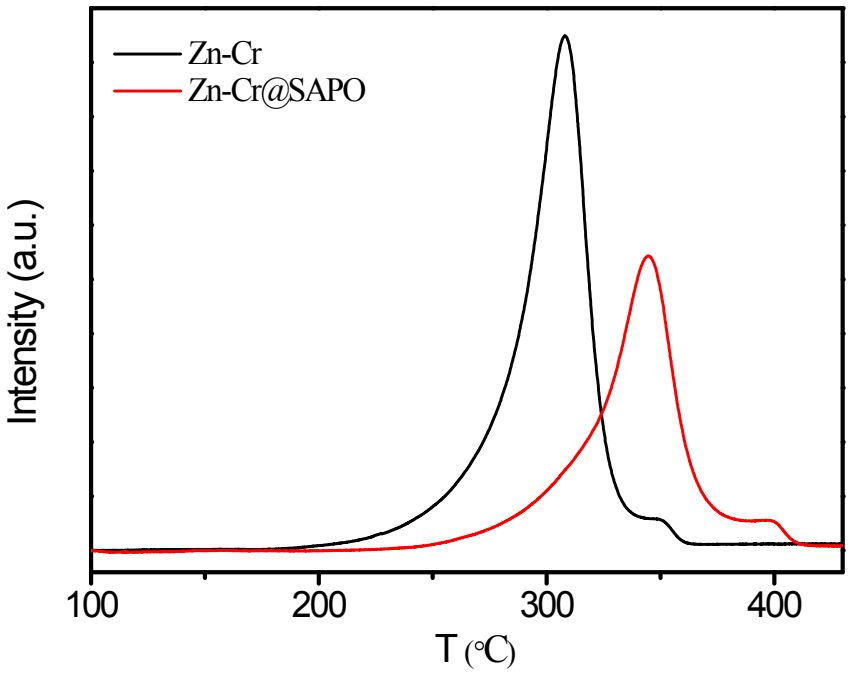

Figure S1. H_2-TPR of Zn-Cr metallic oxide and capsule catalysts.

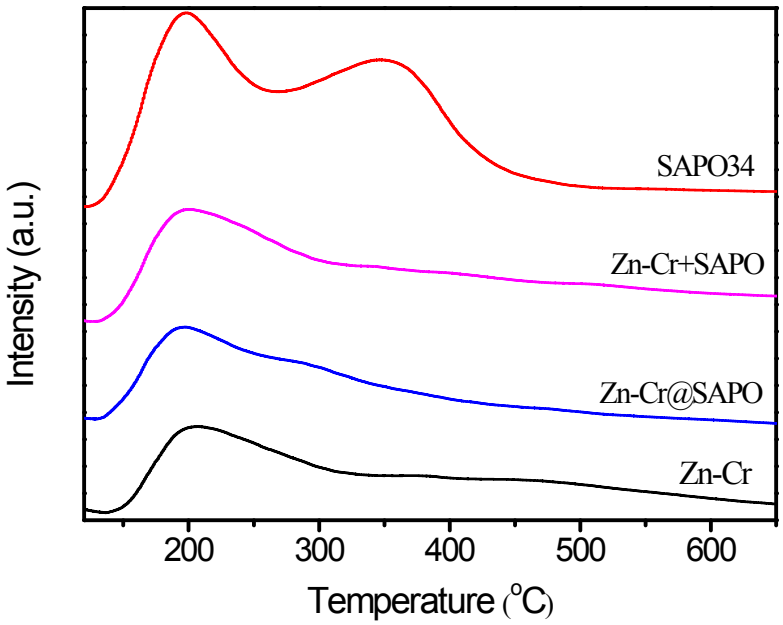

Figure S2. NH_3-TPD of various samples.

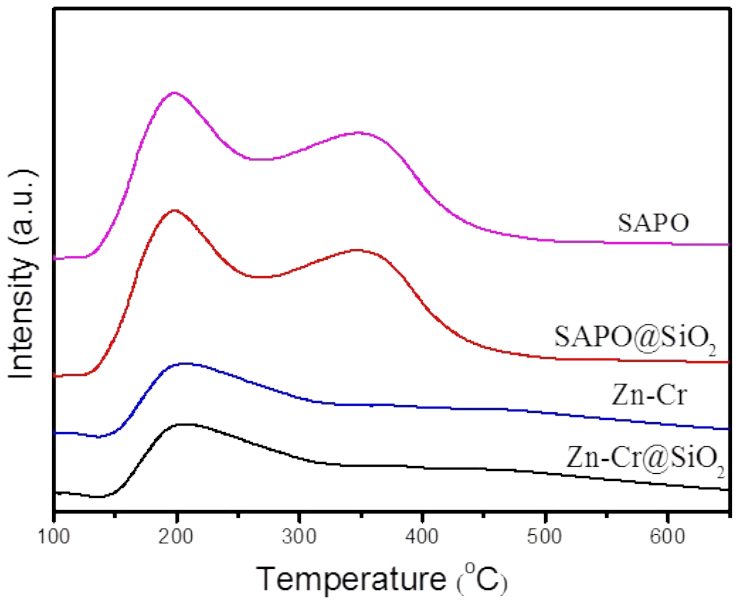

Figure S3. NH_3-TPD of the catalysts modified by diluted silica sol.

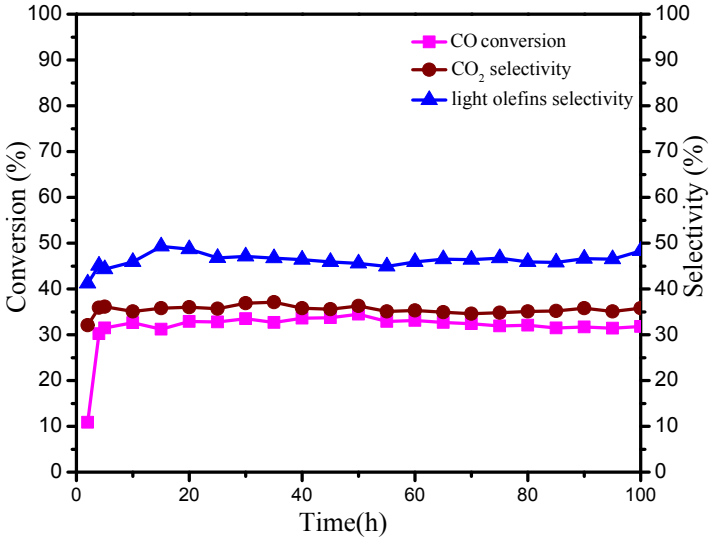

Figure S4. The stability of Zn-Cr@SAPO capsule catalyst in the light olefins synthesis reaction. Reaction condition: $H_2/CO=2.0$, P=2.0 MPa, T=400 °C, Space velocity=2160 $cm^3h^{-1}g_{cat}^{-1}$. The weight ratio of ZnCr and SAPO is 4:1.

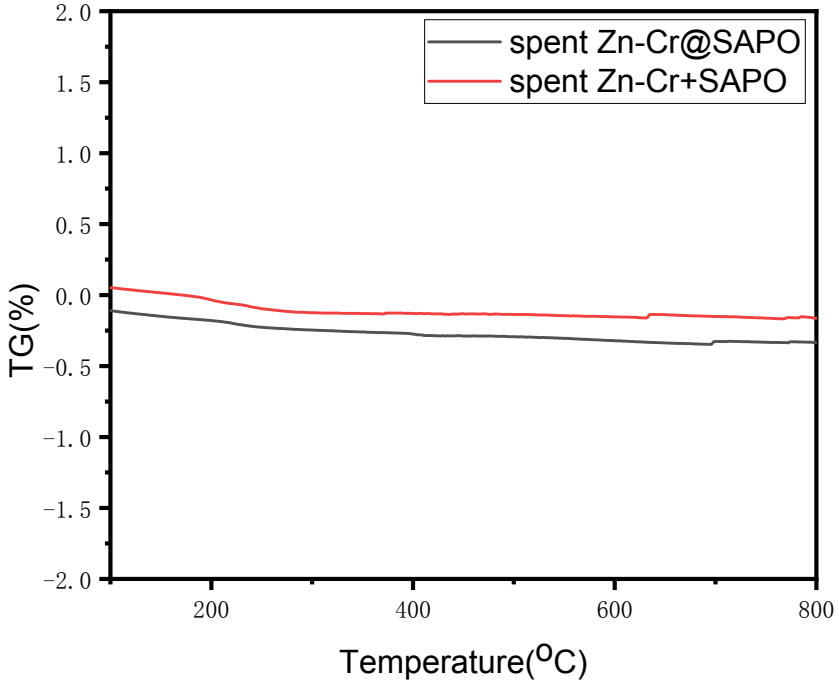

Figure S5. TG results for the spent catalysts.

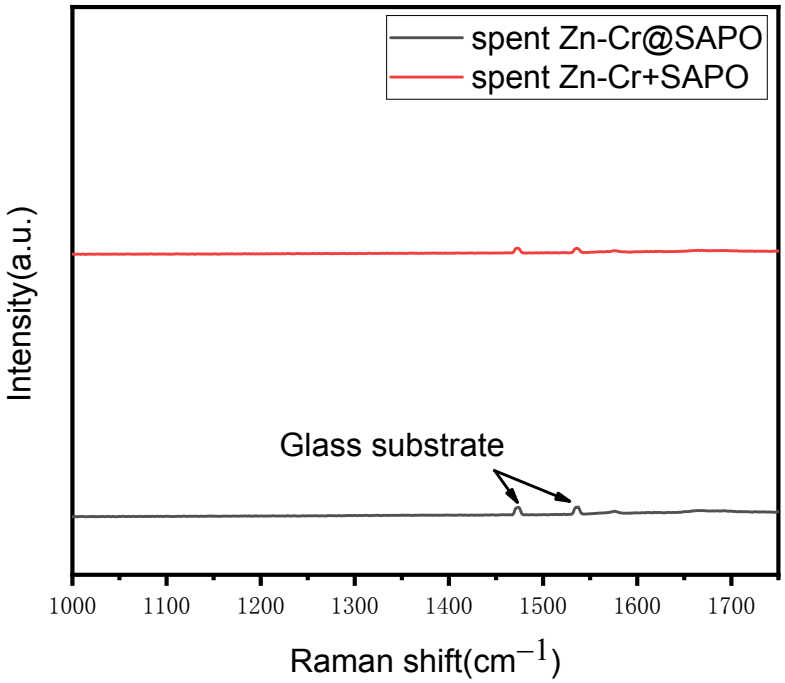

Figure S6. Raman spectra for the spent catalysts.

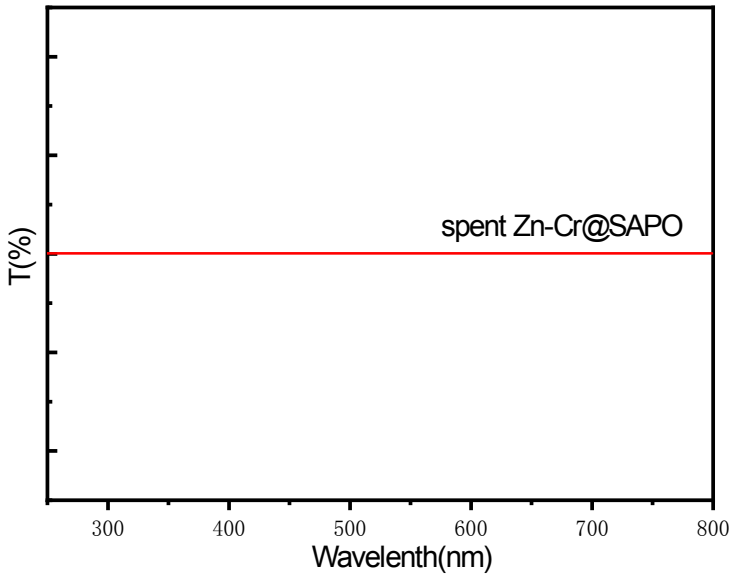

Figure S7. UV-Vis spectra of the spent capsule catalyst.

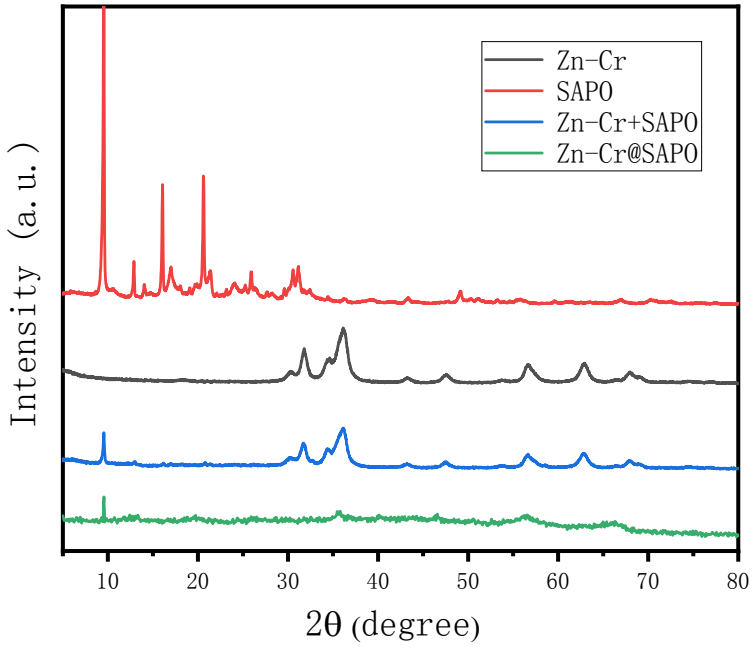

Figure S8. XRD patterns of Zn-Cr catalyst, SAPO-34 zeolite, Zn-Cr and SAPO physical mixture catalyst, Zn-Cr@SAPO capsule catalyst.

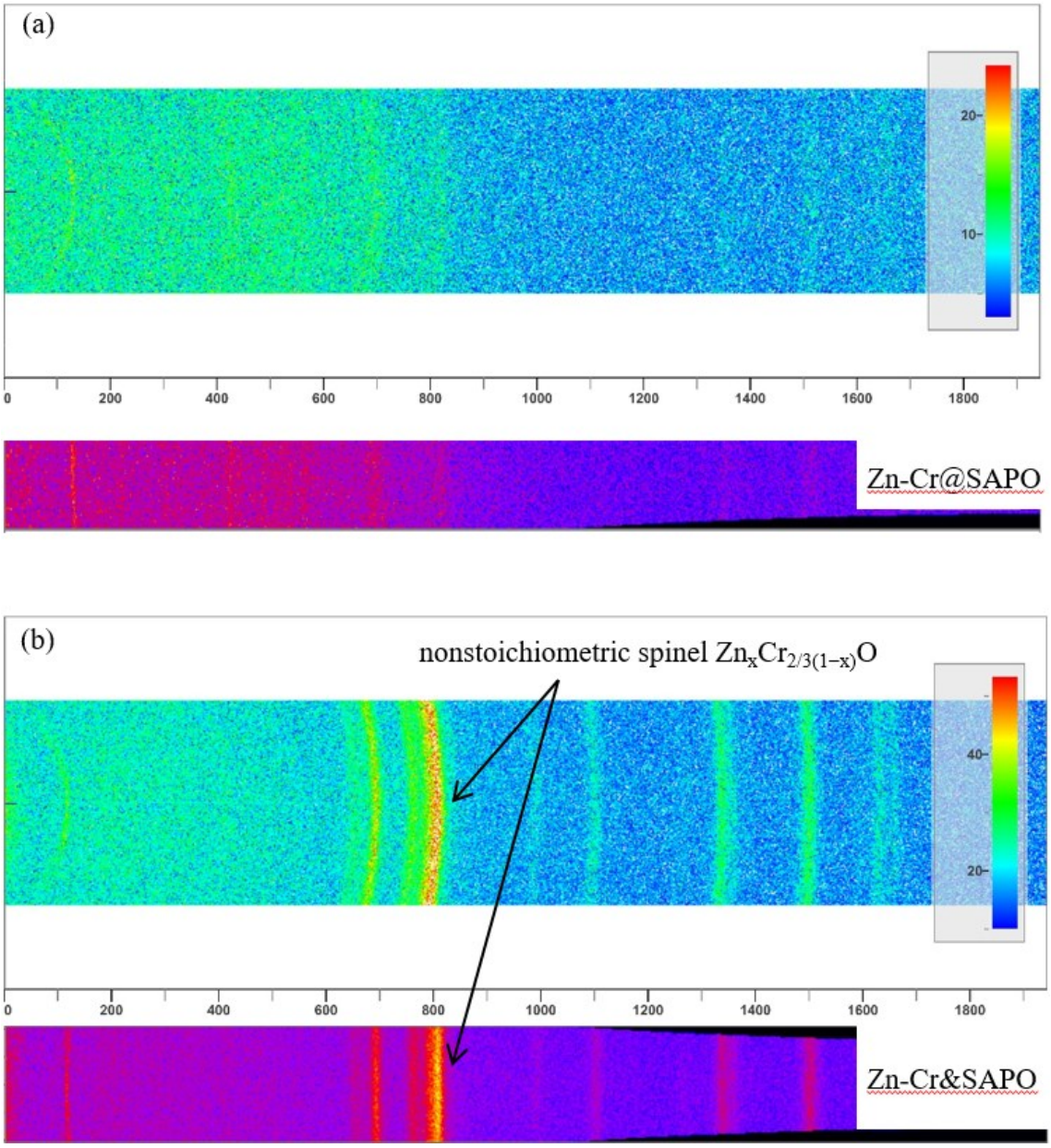

Figure S9. 2D-XRD images of Zn-Cr@SAPO capsule (a) and Zn-Cr+SAPO physical mixture (b) catalysts.

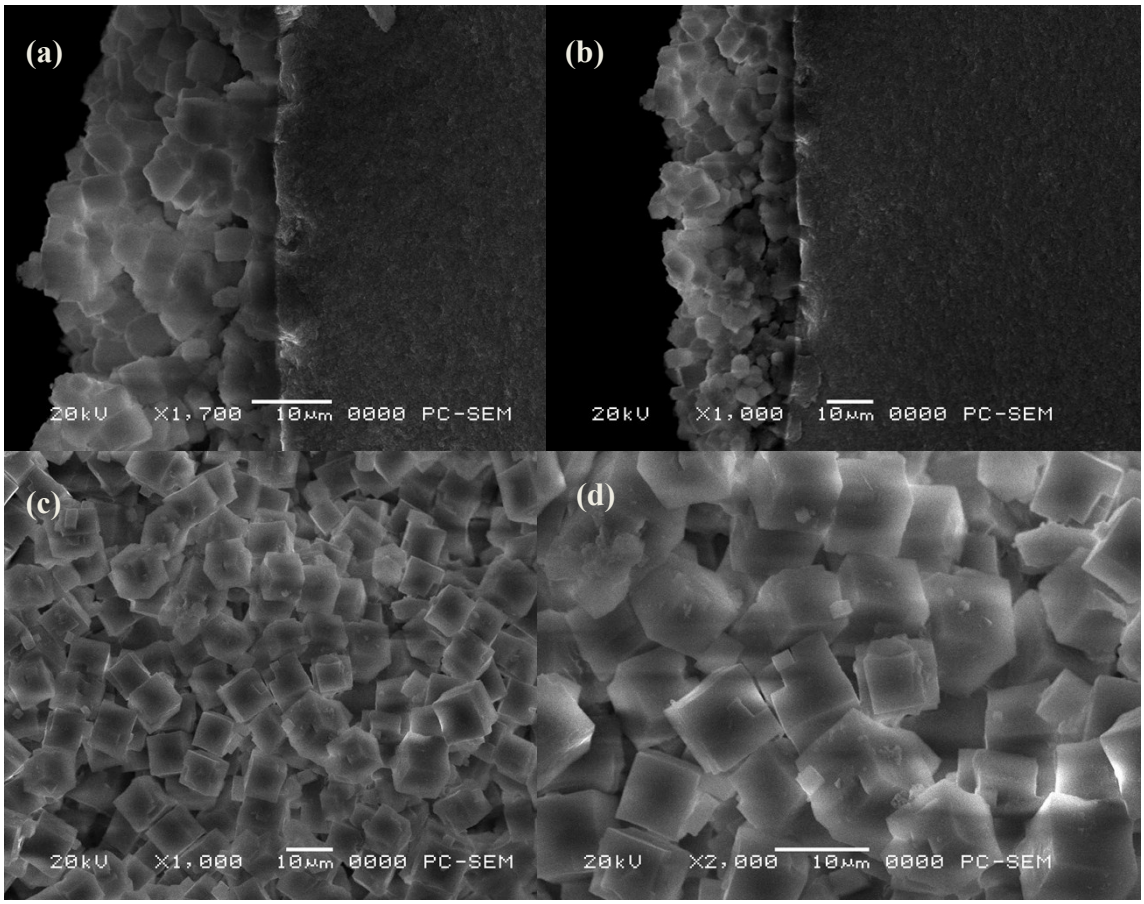

Figure S10. The SEM images of section of Zn-Cr@SAPO capsule catalyst (a, b) and the surface of SAPO34 zeolite (c, d).

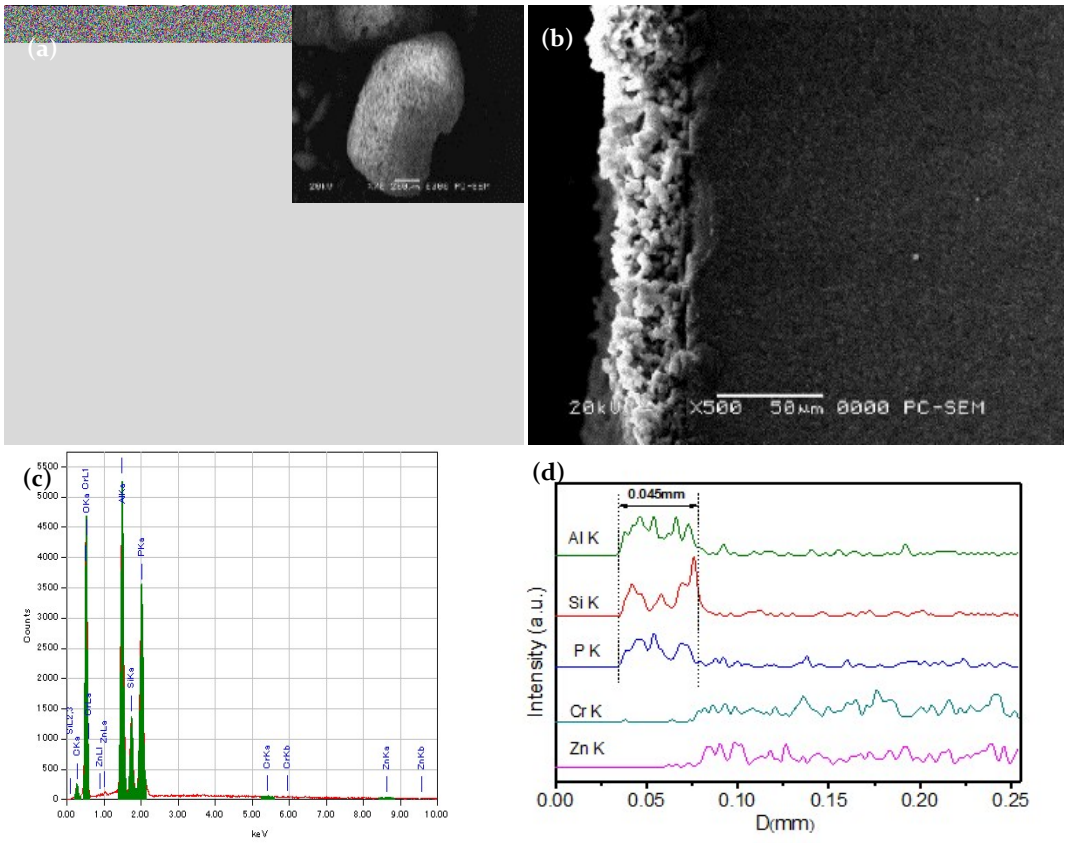

Figure S11. The SEM images (inset: morphology under lower magnification) of (a) the surface of Zn-Cr@SAPO catalyst, (b) section of Zn-Cr@SAPO catalyst, and EDS analysis of (c) surface of Zn-Cr@SAPO, (d) Zn-Cr@SAPO catalyst (linear scanning of section).

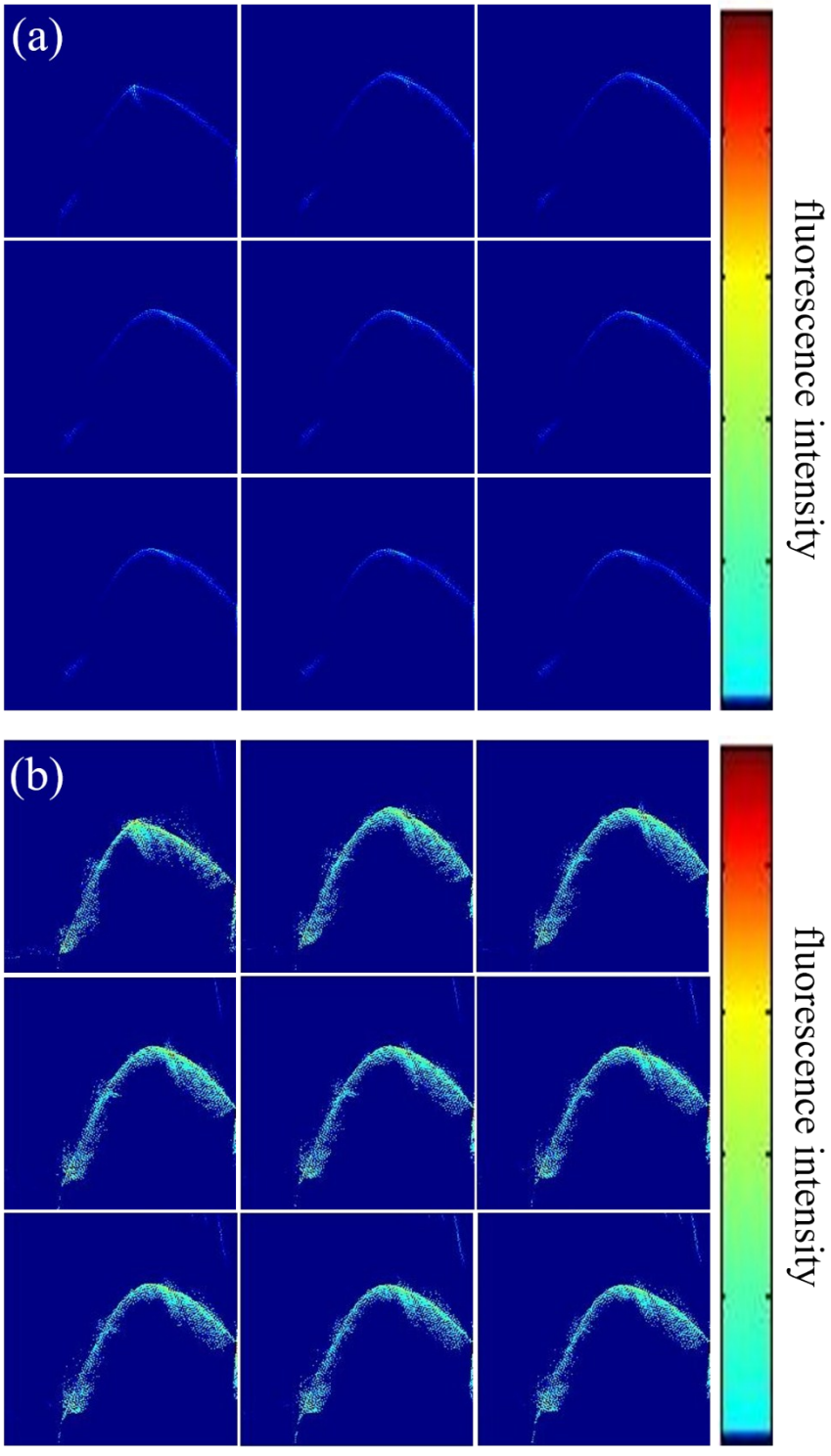

Figure S12. The fluorescence intensity images of Cr (a) and Zn (b) elements of Zn-Cr@SAPO capsule catalyst in 9 different positions.

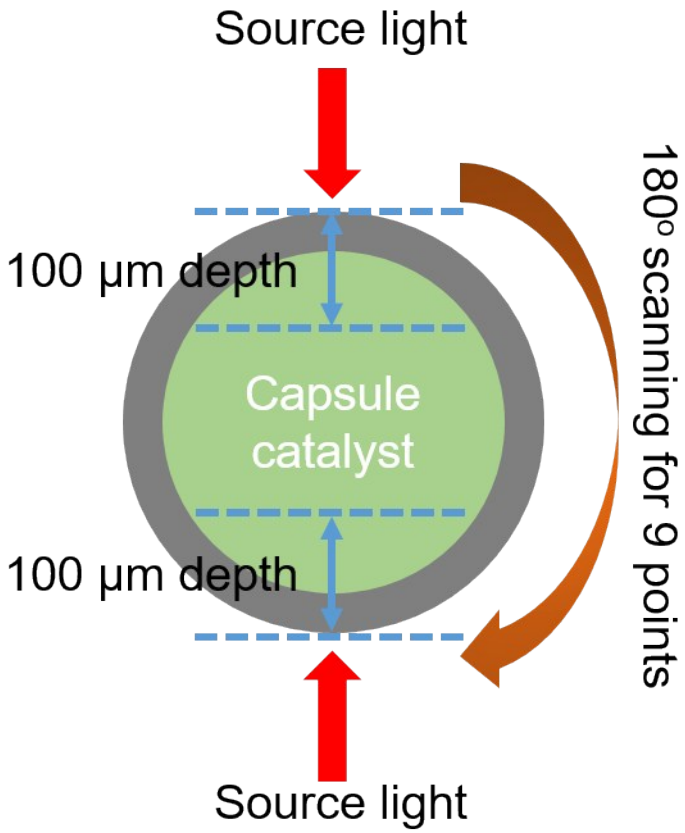

Figure S13. The diagram of XRF-CT method for Zn-Cr@SAPO capsule catalyst studying.

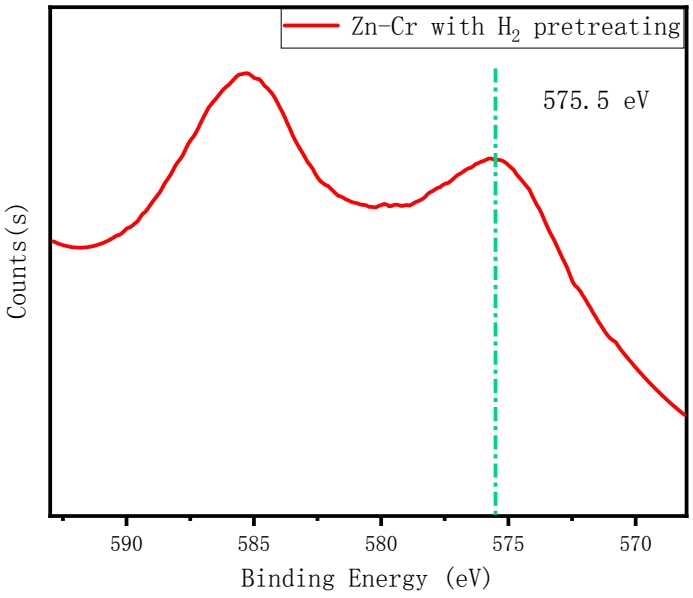

Figure S14. XPS Cr2p spectra of Zn-Cr catalyst after H_2 activation in prior to reaction.

Table S7. The concentration of OH, O_{defect} and $O_{lattice}$ in Zn-Cr catalyst.

Catalyst	OH (%)	O_{defect} (%)[a]	$O_{lattice}$ (%)	$O_{defect}/O_{lattice}$
Zn-Cr(fresh)	21.56	34.61	43.83	0.79
Zn-Cr (activated)	63.74	33.49	2.77	12.09

[a] The O_{defect} concentration is the fraction of surface oxygen atoms adjacent to a defect calculated from the de-convoluted O1s XPS signal.

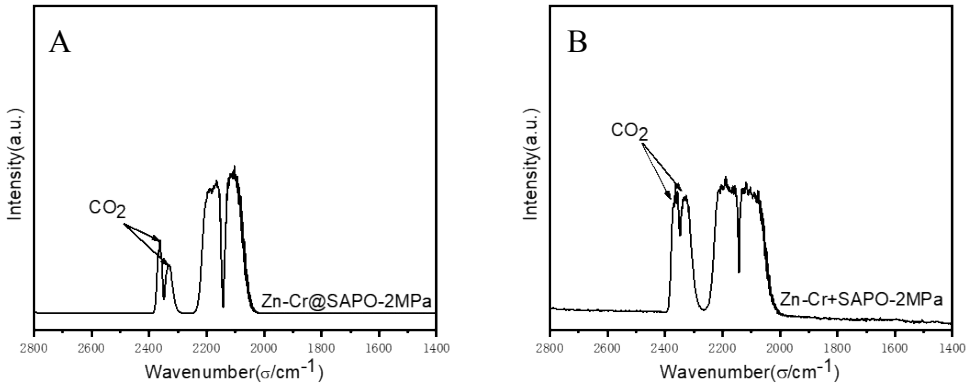

Figure S15. DRIFTS spectra of the physical mixture and capsule catalysts under reaction condition with a flow of syngas at 2.0 MPa, 400 °C.

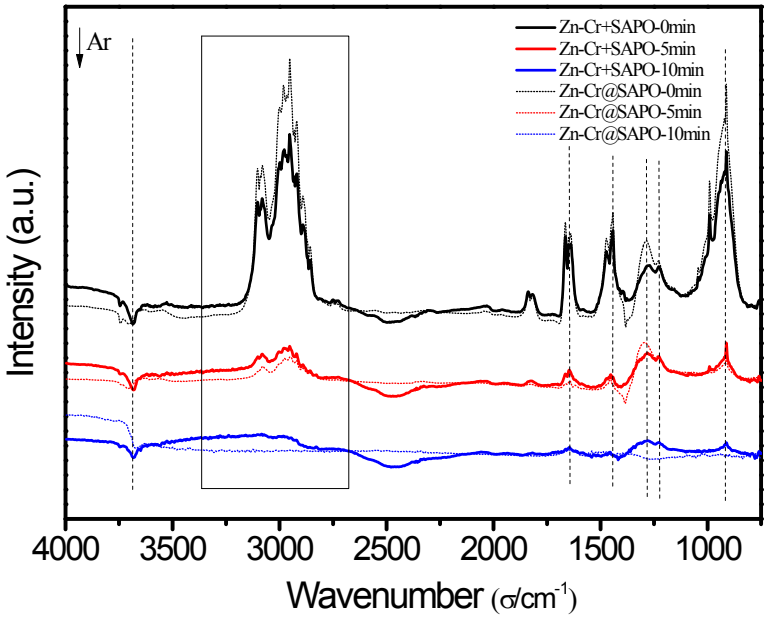

Figure S16. In situ FT-IR spectra of the physical mixture and capsule catalysts. The catalysts were absorption by propylene, then under a flow of Ar for 10 min at 300 °C.

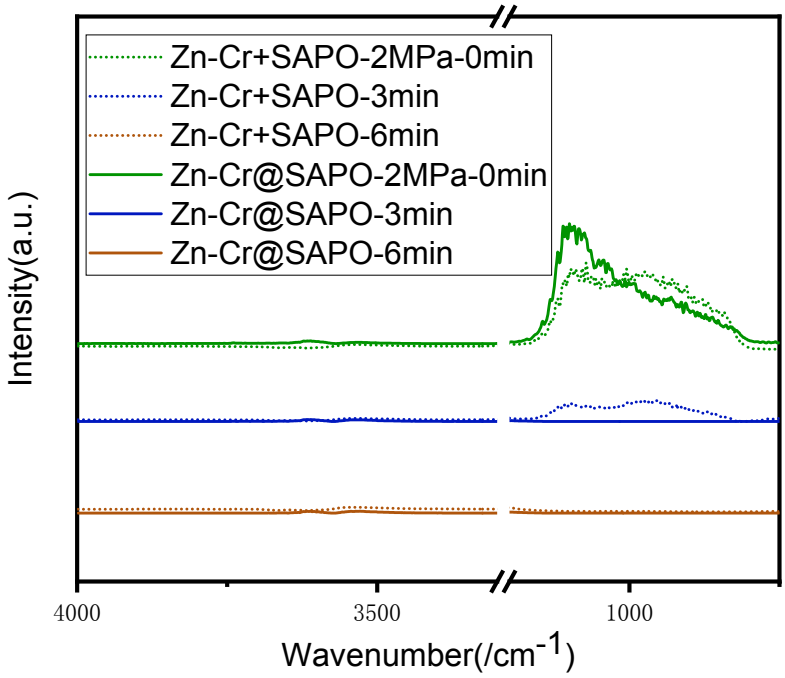

Figure S17. In situ FT-IR spectra of the mixture and capsule catalysts. The catalysts were absorbed by ethylene under reaction condition of 2.0 MPa, 400 °C, followed by rapidly releasing pressure, then under a flow of Ar for 6 min. The Figure S17 and S18 show light olefin is more easily removed from Zn-Cr@SAPO capsule catalyst. Herein, the hydrogenation of light olefins is limited since the core-shell structure, which leads to an increase of light olefins selectivity in STO synthesis.

References

[1] P.E. Blöchl, *Phys. Rev. B.* **1994**, *50*, 17953–17979.

[2] J.P Perdew, K. Burke, *M. Phys. Rev. Lett*. **1996**, *77*, 3865−3868.

[3] C.J. Cramer, In Essentials of Computational Chemistry: Theories and Models, 2nd ed.; Wiley & Sons: Chichester, U.K., **2004.**